Precision of determining bone pose and marker position in the foot and lower leg from computed tomography scans

How low can we go in radiation dose?

Schallig, W.; van den Noort, J. C.; Kleipool, R. P.; Dobbe, J. G.G.; van der Krogt, M. M.; Harlaar, J.; Maas, M.; Streekstra, G. J.

DOI
10.1016/j.medengphy.2019.05.004

Publication date
2019

Document Version
Final published version

Published in
Medical Engineering and Physics

Citation (APA)
Schallig, W., van den Noort, J. C., Kleipool, R. P., Dobbe, J. G. G., van der Krogt, M. M., Harlaar, J., Maas, M., & Streekstra, G. J. (2019). Precision of determining bone pose and marker position in the foot and lower leg from computed tomography scans: How low can we go in radiation dose? *Medical Engineering and Physics*, *69*, 147-152. https://doi.org/10.1016/j.medengphy.2019.05.004

Medical Engineering and Physics 69 (2019) 147–152

Contents lists available at ScienceDirect

Medical Engineering and Physics

journal homepage: www.elsevier.com/locate/medengphy

Technical note

Precision of determining bone pose and marker position in the foot and lower leg from computed tomography scans: How low can we go in radiation dose?

W. Schallig[a,b,*], J.C. van den Noort[a,b], R.P. Kleipool[c], J.G.G. Dobbe[d], M.M. van der Krogt[a], J. Harlaar[a,e], M. Maas[b], G.J. Streekstra[b,d]

[a] Amsterdam UMC, Vrije Universiteit Amsterdam, Rehabilitation Medicine, Amsterdam Movement Sciences, De Boelelaan 1117, Amsterdam, the Netherlands
[b] Amsterdam UMC, University of Amsterdam, Radiology and Nuclear Medicine, Musculoskeletal Imaging Quantification Center (MIQC), Amsterdam Movement Sciences, Meibergdreef 9, Amsterdam, the Netherlands
[c] Amsterdam UMC, University of Amsterdam, Medical Biology, Amsterdam Movement Sciences, Meibergdreef 9, Amsterdam, the Netherlands
[d] Amsterdam UMC, University of Amsterdam, Biomedical Engineering and Physics, Amsterdam Movement Sciences, Meibergdreef 9, Amsterdam, the Netherlands
[e] Delft University of Technology, Department of Biomechanical Engineering, Delft, the Netherlands

ARTICLE INFO

Article history:
Received 7 February 2019
Revised 29 March 2019
Accepted 13 May 2019

Keywords:
Computed tomography
Dose reduction
Biomechanics
Foot
Movement analysis
Skin-mounted markers
Segmentation
Registration

ABSTRACT

Computed tomography (CT) imaging can be used to determine bone pose, sometimes combined with skin-mounted markers. For this specific application, a lower radiation dose than the conventional clinical dose might suffice. This study aims to determine how lowering the radiation dose of a CT-scan of the ankle and foot affects the precision of detecting bone pose and marker position. Radiation dose is proportional to tube charge. Hence, an adult cadaveric leg was scanned 10 times at four different tube charges (150, 75, 50 and 20 mAs) with a Philips Brilliance 64 CT scanner. Precision of detecting bone and marker position at 50 mAs was not significantly different from 75 mAs and from the clinically used 150 mAs, but higher than 20 mAs. Furthermore, no differences of the precision in detecting bone orientation were found. These results indicate that the radiation dose can be reduced by a factor 3 compared to the clinically usual radiation dose, without affecting the precision of detecting bone pose and marker position in the foot and ankle.

1. Introduction

In the field of orthopedic and biomechanical research, computed tomography (CT) scans can be used to determine the pose (i.e. position and orientation) of bones. For the foot specifically, information about the bone pose has been used for instance to quantify subtalar joint motion [1,2], to evaluate axial loading during scanning in hallux valgus patients [3], to evaluate the effect of ankle braces [4] and to develop subject-specific musculoskeletal models for application in movement analysis [5,6].

Several studies used CT scans in combination with markers attached to the skin [7–11]. Generally, these studies aim to evaluate movement analyses, for instance by means of kinematic validation [7,8] or the determination of joint centers [9]. Skin markers, which are used during motion tracking are assumed to represent the underlying bony structures in both static and dynamic conditions. However, in dynamic conditions like gait, relative motion occurs between skin-mounted markers and corresponding bones of the lower leg and foot, known as soft tissue artifacts due to skin and other soft tissue movement [12–15]. These artifacts affect the relation between the marker-based coordinate system and the bone-embedded coordinate system, and thus limit the accuracy of the estimation of bone kinematics. A CT scan protocol in which the pose of bones and the position of skin-mounted markers are recorded, will enable to quantify these soft tissue artifacts albeit not in dynamic, but in multiple static conditions (i.e. a series of scans).

Although CT is the most appropriate technique for imaging bones, the scanned individuals are exposed to radiation. The increasing use of CT scans over the last decades has raised the interest in lowering the radiation dose of scans [16–18]. Tube current is considered as the most practical acquisition setting to alter when aiming for a lower radiation dose [16]. The tube charge (i.e. tube

* Corresponding author at: Amsterdam UMC, Vrije Universiteit Amsterdam, Rehabilitation Medicine, Amsterdam Movement Sciences, De Boelelaan 1117, 1081 HV Amsterdam, the Netherlands.
E-mail address: w.schallig@vumc.nl (W. Schallig).

https://doi.org/10.1016/j.medengphy.2019.05.004
1350-4533/

current-time product) is directly proportional to the radiation dose [19]. However, image noise is inversely proportional to the square root of the radiation dose [19]. Hence, a lower radiation dose reduces the image quality, which might affect the precision of detecting bone pose and marker position.

The effect of lowering the radiation dose from a clinically used dose on the precision of detecting bone pose has been studied in for example the wrist [20]. However, these results cannot be directly translated to other joints because of a different anatomy. To our knowledge, it is unknown whether the tube charge (i.e. radiation dose) can be reduced compared to the frequently used 150 mAs [2,4,21–23], when detecting the pose of bones in the foot and ankle. In a series of scans, the first scan is the so called segmentation scan, which is often acquired at around a tube charge of 150 mAs, to yield a segmentation of each object (i.e. bone or marker). Then these segments are registered (i.e. matched) to subsequent low-dose CT-scans (20–25 mAs). Hence, lowering the radiation dose of the segmentation scan can also influence the precision of the registration output, which also has not yet been studied for the foot and ankle. Furthermore, the precision of detecting the position of skin-mounted markers in a CT-scan has not yet been described, even though such markers are frequently used in CT-scans [7–11].

Therefore, the main aim of this study is to determine how lowering the radiation dose of a CT-scan of the ankle and foot affects the precision of detecting the bone pose. The secondary aim is to determine how lowering the radiation dose affects the precision of detecting the position of skin-mounted markers and consequently the orientation of a marker-based coordinate system. This study focuses on lowering the tube charge of the high-dose segmentation scan in a series of scans and its effect on the precision of detecting bone pose and marker position after segmentation and after registration.

2. Materials and methods

2.1. Experimental setup

A freshly frozen cadaveric left lower leg from a 70 years old male was used for this study. A CT scan of the lower leg was evaluated by a musculoskeletal radiologist (MM) to rule out pathology or former surgery. Thirteen skin-mounted markers with a diameter of 14.0 mm were placed on the foot and lower leg. These passive markers are plastic balls covered with reflective tape and have a hard plastic base. Normally these markers are used for 3D gait analysis with a VICON system (Vicon Motion Systems Ltd., Oxford, UK), but this material also had a good contrast in a CT image. The locations of the markers (Table 1, Fig. 1) were a selection of three common foot models used in gait analysis [24–26]. After marker placement, the lower leg was placed on the CT table (Brilliance 64 CT scanner; Philips Medical Systems, Best, the Netherlands). A total of 40 scans were obtained from the frozen cadaveric lower leg and foot using a standard CT ankle scanning protocol with the same slice thickness (0.67 mm), increment (0.3 mm), voxel size ($0.3 \times 0.3 \times 0.3$ mm), reconstruction filter (D, which is vendor specific and specifically designed for bones) and tube voltage (120 kV). Only the tube charge was varied over scans, with 10 repetitions per setting. The four different tube charges were 150, 75, 50 and 20 mAs. All scans were used to determine the precision after segmentation and only one segmented scan of each tube charge was used to perform the registration to all 20 mAs scans (Fig. 2).

2.2. Segmentation procedure

The 10 foot and lower leg bones and 13 skin mounted markers and 10 corresponding foot and lower leg bones (Table 1) were segmented in all 40 scans with custom-made software [27] for each scan separately by the same well trained researcher.

In short, the 3D segmentation procedure of the software started with threshold-connected region growing [28] in which a starting point was identified manually in the cortical bone. In this procedure, connected neighboring voxels, with an intensity in a user-specified range, were added automatically until the selection was considered as satisfactory. Next, a binary closing operation was used [29] to fill remaining gaps and for closing of the outline. At this point, voxels could be added manually using a painting brush. Subsequently, a Laplacian level-set segmentation algorithm [28] was used to advance the selection toward a more accurate outline of the bone. This segmentation result was used to produce a polygon mesh by applying the marching cubes algorithm [30]. Each point of this polygon mesh was assigned a gray level of the accompanying CT image, which was used for registration (described below).

For every single scan, the segmentation provided a geometrical model of the object. The object position was defined by the centroid of the points describing the polygon model, assuming an equal distribution of mass over the bone or marker. The orientation of each bone was calculated based on the principal axes of inertia of the segmented bone in reference to the CT-based coordinate system. In addition, one marker-based coordinate system was constructed as described in detail below, to investigate the effect of lowering the tube charge on the orientation of a marker-based coordinate system.

Table 1
Segmented bones and markers and their location.

Bones	Markers	Marker location
Tibia	MMAL	Medial Malleolus
Fibula	LMAL	Lateral Malleolus
Calcaneus	MCAL	Medial side of the calcaneus
	LCAL	Lateral side of the calcaneus
	CALP	Posterior aspect of the calcaneus
Cuboid	–	–
Navicular	–	–
Metatarsal 1	HM1	Head of Metatarsal 1
	HM1M	Head of Metatarsal 1 medial side
	BM1	Basis of Metatarsal 1
Metatarsal 2	HM2	Head of Metatarsal 2
	BM2	Basis of Metatarsal 2
Metatarsal 5	HM5	Head of Metatarsal 5
	BM5	Basis of Metatarsal 5
Proximal Phalanx 1	–	–
Distal Phalanx 1	NHAL	Nail of the hallux

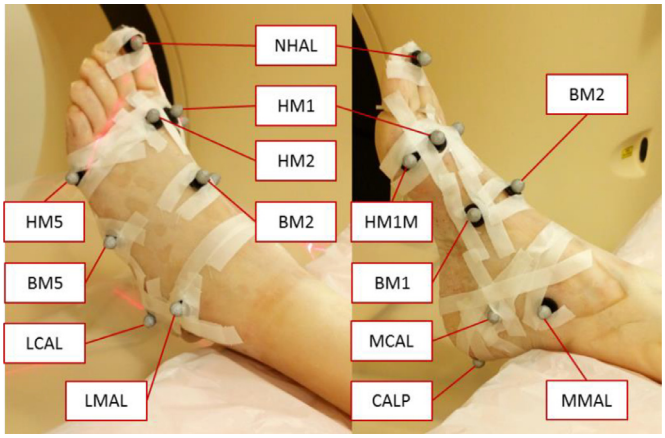

Fig. 1. The cadaveric lower leg and foot with skin-mounted markers in the CT scanner. The marker abbreviations are explained in Table 1. The tape was needed to secure the adhesion of the markers to the frozen specimen.

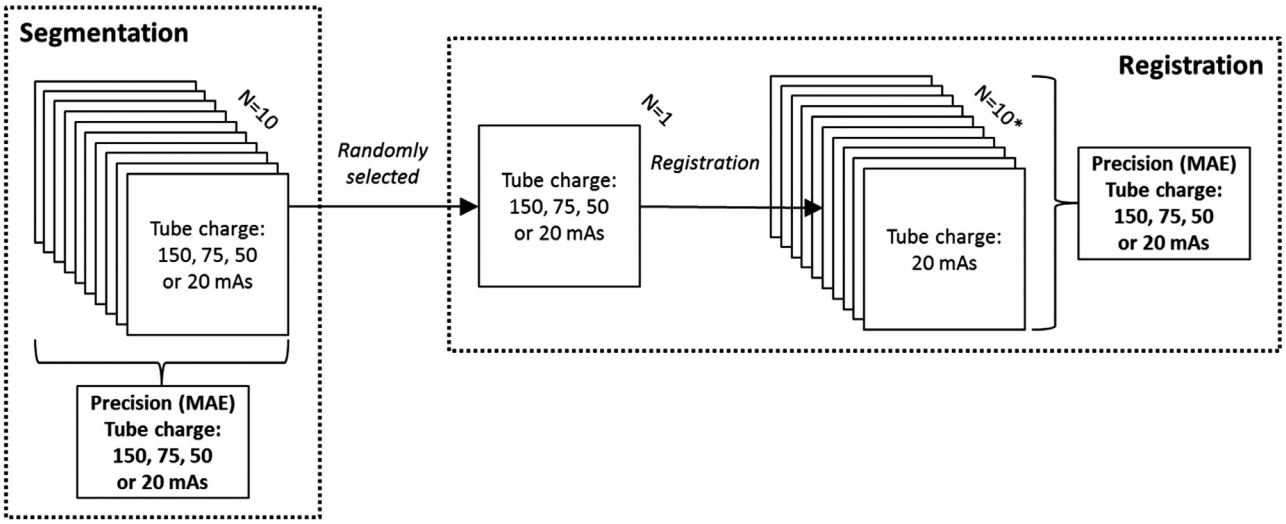

Fig. 2. Overview of which scans are used for the segmentation and which for the registration procedure. MAE is the mean absolute error, which is the measure for precision used in this study. N = the amount of CT scans. *When the tube charge of the segmented scan is 20 mAs, $N = 9$ because one scan is used as segmentation scan.

2.3. Registration procedure

Registrations were performed to determine the bone poses and marker positions in a series of scans. Generally, a scan that is used for registration can be of a lower dose than the segmentation scan. Hence, in this study, the scans acquired at 20 mAs scans were used for registration. One randomly selected scan of every tube charge (i.e. 150, 75, 50 and 20 mAs) was considered as segmentation scan and matched to the 20 mAs scans (Fig. 2). This means that 39 registrations were performed. Ten for the 150, 75 and 50 mAs scans and nine for the 20 mAs scans since the randomly selected 20 mAs scan could not be registered to itself.

The same custom-made software as used for the segmentation was also used for the registration [27]. The automatic registration procedure of the software was first manually initialized. After this initialization step, a Nelder–Mead [31] downhill simplex optimizer algorithm was used to optimize the correlation coefficient between the gray-levels assigned to the polygon points during segmentation, and a target gray-level image.

Each registration provided a transformation matrix representing the change in bone pose and marker position relative to the segmentation scan. Also after registration, a marker-based coordinate system was constructed from the marker positions.

2.4. Marker-based coordinate system

As skin-mounted markers are normally used to construct coordinate systems, a coordinate system was constructed in this study to investigate the effect of lowering the radiation dose on the precision of detecting this coordinate system. A coordinate system for the forefoot was used in this study constructed according to the Oxford Foot Model (OFM) definitions [24]. The orientation of the marker-based coordinate system was expressed in the coordinate system of the CT scan.

2.5. Data analysis

The precision in detecting bone pose or marker position was calculated for every tube charge after segmentation and after registration. The precision of the bone pose was described as the precision in position and orientation separately. The precision of the markers was only calculated for the position. In addition, the precision of a marker-based coordinate system was calculated.

All precision measures were expressed as mean absolute error (MAE) for every bone and marker separately. MAE was based on the *x, y* and *z* values of the position (mm) and the rotation around *x, y* and *z* axis for the orientation (degrees), which were provided by the segmentation or registration. The MAE was calculated for every tube charge for each bone or marker as follows (Eq. (1)): (I) the average value over 10 scans in *x, y* and *z* direction was determined; (II) the mean was subtracted from each individual value, to make the MAE independent from the location of the bone or marker in the scanner; (III) the error of each scan was calculated by taking the norm from the absolute *x, y* and *z* values [32]; (IV) the average value was taken over the 10 error values, resulting in a mean absolute error (in mm or degrees).

$$Mean\ Absolute\ Error = \sum_{i=1}^{10} \frac{\sqrt{\left((Xi-\bar{X})^2+(Yi-\bar{Y})^2+(Zi-\bar{Z})^2\right)}}{10} \quad (1)$$

2.6. Statistical analysis

Repeated measures ANOVAs with Bonferroni correction for multiple testing were used to compare the MAE between the four tube charges. Three ANOVAs were performed on both the MAEs of the segmentation and the MAEs of the registration (dependent variable): one for the precision of the position of the bones, one for the precision of the orientation of the bones and one for the precision of the position of the markers. Tube charge was the within-bone or within-marker factor (independent variable). No statistical test was performed for the precision of the orientation of the marker-based coordinate system, because the orientation of only one coordinate system (i.e. the forefoot) was constructed, resulting in one MAE value per tube charge. When performing the ANOVAs, the assumption of sphericity was checked using the Mauchly's test. In the case of a violation of this assumption, the Greenhouse–Geisser or Huynh–Feldt adjustment was performed, based on the Greenhouse–Geisser epsilon [33]. Statistical significance was accepted at $P < 0.05$. All analyses were performed using SPSS statistical software (SPSS 21.0, SPSS Inc., 192 Chicago, IL, USA).

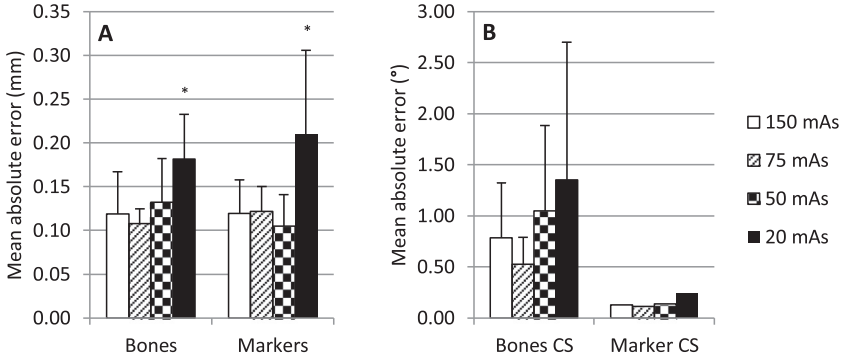

Fig. 3. The precision as expressed by the mean absolute error of the position (A) and orientation (B) of the bones and marker-based coordinate system after segmentation. Error bars show the standard deviation over all the 10 bones or 13 markers. No error bars are present for the marker-based coordinate system, because only one coordinate system was reconstructed. *Significantly different from 150, 75 and 50 mAs.

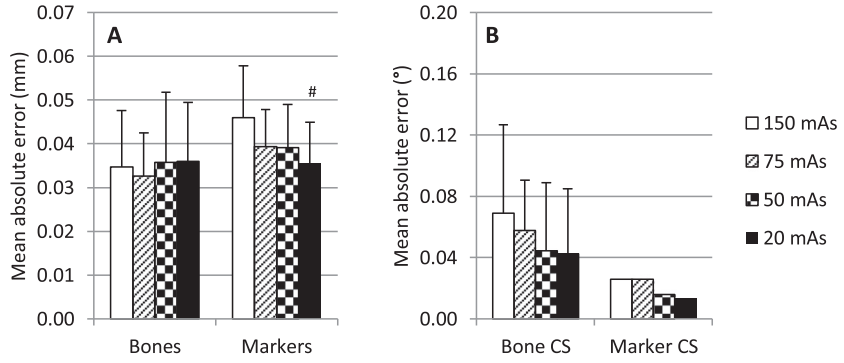

Fig. 4. The precision as expressed by the mean absolute error of the position (A) and orientation (B) of the bones and marker-based coordinate system after registration. Error bars show the standard deviation over all the 10 bones or 13 markers. Note that the *y*-axis is 5 times smaller in A and 15 times smaller in B compared to Fig. 3(A) and (B). No error bars are present for the marker-based coordinate system, because only one coordinate system was reconstructed. #Significantly different from 150, and 75 mAs.

3. Results

3.1. Segmentation

The MAEs of the position of all bones and markers after segmentation are shown in Fig. 3(A). A significant main effect of tube charge was found on the MAE of the position of the bones ($F = 11.00$, $P < 0.001$) and the markers ($F = 11.80$, $P < 0.01$) after segmentation. Post-hoc analysis showed a significantly higher MAE for the 20 mAs scans compared to the other three tube charges for both bones (Diff: 0.05–0.07 mm) and markers (Diff: 0.09–0.11 mm). No statistical differences were found between the other three tube charges, of which the MAEs were all below 0.15 mm.

The MAEs of the orientation of bones and a marker-based coordinate system after segmentation are shown in Fig. 3(B). Although a significant main effect of tube charge was found for the MAE of the orientation of bones ($F = 5.11$, $P = 0.03$), no significant differences were shown in the post-hoc analysis. The MAE of the orientation of the marker-based coordinate system was similar for 150, 75 and 50 mAs scans (0.11°–0.14°), but higher for the 20 mAs scans (0.24°).

3.2. Registration

The MAEs of the position of bones and markers after registration are shown in Fig. 4(A). No significant main effect of tube charge was found for the bones. A statistically significant main effect of tube charge was found for the MAE of the position of the markers after registration ($F = 11.49$, $P < 0.01$). Post-hoc analysis showed a significantly lower MAE of the 20 mAs scans compared to the 150 and 75 mAs scans (Diff: 0.004–0.01 mm).

Average MAE values of the orientation of coordinate systems based on bone geometry and on a set of markers after registration are shown in Fig. 4(B). No significant main effect of tube charge was found on the orientation of the bones after registration. MAE of the orientation of the marker-based coordinate system was below 0.03° for all tube charges and for 20 mAs even below 0.015°.

4. Discussion

The aim of this study was to determine how lowering the radiation dose of a CT-scan of the ankle and foot affects the precision of detecting the bone pose, the position of skin-mounted markers and consequently the orientation of a marker-based coordinate system. The main finding was that the precision values were not different between 150, 75 and 50 mAs scans, but the 20 mAs scans showed a significant higher MAE (i.e. a lower precision) for the position of both bones and markers after segmentation.

These findings indicate that the tube charge of CT scans of the foot and ankle can be lowered from the frequently used 150 mAs [2,4,21–23] to 50 mAs, without losing precision in determining bone pose and marker position. The main reason to lower the tube charge of the scans is to lower the radiation dose to the subject. The tube charge is directly proportional to the radiation dose [19], hence this study shows that the dose can be reduced by a factor of 3 (from a CT dose index of 12.5 mGy to 4.2 mGy) when reducing the tube charge from clinically used 150 mAs to 50 mAs. Despite the significantly higher MAE for the 20 mAs scans, even these

scans can be considered to be used for the segmentation, since the MAE is still below 0.3 mm for the position and in the order of 1.5° for the orientation. A second benefit that comes with lowering the dose is that the scanning device will heat up less and will operate more stable over a longer period of time.

This study shows that studies with bone pose as outcome measure [1–6] can determine this measure with a MAE of 0.13 mm for the position and 0.70° for the orientation after segmentation of a 50 mAs scan and a MAE of less than 0.04 mm for the position and 0.05° for the orientation after registration to a 20 mAs scan. The registration MAE is considerably lower than the segmentation MAE, which indicates that studies which make use of a series of scans [1–4,22,23], could use 20 mAs scans for the registration scans without adding any noteworthy precision error (<0.05 mm; <0.1°) to the total error as sum of registration and segmentation. Therefore, in a series of scans, multiple registration scans of 20 mAs can be used. This will result in a much lower radiation dose compared to the same amount of scans with a tube charge of 150 mAs [22].

To our knowledge, current literature did not yet describe the precision of detecting the position of skin-mounted markers in a CT-scan, even though these markers are frequently used in CT-scans [7–11]. This study shows that the precision of detecting the position of skin-mounted markers after segmentation was similar as for bones and had an average MAE value of 0.10 mm when scanning at 50 mAs. The typical use of the markers is within motion tracking. Interestingly, the average MAE of detecting the marker positions in this study was even lower compared to the measurement error of markers by a motion capture system (0.15 mm) [34]. Marker positions are often used to construct coordinate systems of body segments, which are then used to calculate joint angles. In this study, the MAE of the orientation of the marker-based coordinate system of the forefoot after segmentation was 0.14°, which is lower than the MAE of the bones. This might be because the marker-based coordinate system is based on the center of the markers, while the orientation of the bones is based on the axes of inertia and therefore more susceptible for the variation in segmentation. The MAE of the registration of the markers was surprisingly higher for 20 mAs scans compared to the other tube charges. However, since the values are all lower than 0.05 mm and much smaller compared to the errors after segmentation, it is therefore probably not going to lead to a clinically relevant difference.

Magnetic resonance imaging can be an alternative for CT imaging. It does not involve ionizing radiation and it has also been used in motion analysis studies [35,36]. However, CT is the preferred technique and generally used when imaging bones due to the high contrast and well defined borders of bone relative to the surrounding soft tissue. Furthermore, it is cheaper and faster than MRI. Especially in studies that involve skin-mounted markers, a series of scans is often made, which would lead to unacceptable long scanning times in an MRI scanner. Moreover, as this study shows, the effective radiation dose of a CT scan of the foot and ankle is only 0.02 mSv (CT dose index: 4.2 mGy) when scanning at 50 mAs.

Several limitations of the study have to be addressed. Only one 70 years old male cadaveric leg was scanned and analyzed. Including more legs could strengthen the results, however we do not expect a different outcome with respect to the precision differences between the different tube charges. Furthermore, a different scanner might affect the precision values. However, the Brilliance scanner is not a high-end scanner, which means that similar or even higher precision values can be expected for high-end scanners. This expectation is confirmed by the results of a similar study where accuracy and precision of bone pose estimates are quantified as a function of scan parameter settings for a common and a high-end CT-scanner [20]. The use of different software can also affect the precision values. However, the software used in this study has shown a high precision in this study and a high accuracy and precision in previous studies [20,27].

5. Conclusions

Computed tomography scans of the foot and ankle in which bone pose or marker positions are determined, can be performed with a tube charge of 50 mAs. This will lower the radiation dose by a factor 3 compared to the clinically used tube charges, without affecting the precision of detecting bone pose and marker position. Moreover, in a series of scans, the subsequent registration scans can be scanned at a tube charge as low as 20 mAs, lowering the radiation dose even more, without adding a notable error to the total error as sum of registration and segmentation.

Disclosure

The authors do not report any potential conflict of interest.

Funding

This research was funded by an internal grant of the Amsterdam Movement Sciences Research Institute.

Ethical approval

No ethical approval was required for this study.

References

[1] Gondim Teixeira PA, Formery A-S, Jacquot A, Lux G, Loiret I, Perez M, et al. Quantitative analysis of subtalar joint motion with 4D CT: proof of concept with cadaveric and healthy subject evaluation. Am J Roentgenol 2017;208:150–8.
[2] Beimers L, Tuijthof GJ, Blankevoort L, Jonges R, Maas M, van Dijk CN. In-vivo range of motion of the subtalar joint using computed tomography. J Biomech 2008;41:1390–7.
[3] Watanabe K, Ikeda Y, Suzuki D, Teramoto A, Kobayashi T, Suzuki T, et al. Three-dimensional analysis of tarsal bone response to axial loading in patients with hallux valgus and normal feet. Clin Biomech (Bristol, Avon) 2017;42:65–9.
[4] Kleipool RP, Natenstedt JJ, Streekstra GJ, Dobbe JG, Gerards RM, Blankevoort L, et al. The mechanical functionality of the EXO-L ankle brace: assessment with a 3-dimensional computed tomography stress test. Am J Sports Med 2016;44:171–6.
[5] Malaquias TM, Silveira C, Aerts W, De Groote F, Dereymaeker G, Vander Sloten J, et al. Extended foot-ankle musculoskeletal models for application in movement analysis. Comput Methods Biomech Biomed Eng 2017;20:153–9.
[6] Oosterwaal M, Carbes S, Telfer S, Woodburn J, Torholm S, Al-Munajjed AA, et al. The Glasgow–Maastricht foot model, evaluation of a 26 segment kinematic model of the foot. J Foot Ankle Res 2016;9:19.
[7] Dal Maso F, Blache Y, Raison M, Lundberg A, Begon M. Glenohumeral joint kinematics measured by intracortical pins, reflective markers, and computed tomography: a novel technique to assess acromiohumeral distance. J Electromyogr Kinesiol 2016;29:4–11.
[8] Victor J, Van Glabbeek F, Vander Sloten J, Parizel PM, Somville J, Bellemans J. An experimental model for kinematic analysis of the knee. J Bone Joint Surg Am 2009;91(6):150–63 Suppl.
[9] Michaud B, Jackson M, Arndt A, Lundberg A, Begon M. Determining in vivo sternoclavicular, acromioclavicular and glenohumeral joint centre locations from skin markers, CT-scans and intracortical pins: a comparison study. Med Eng Phys 2016;38:290–6.
[10] McNamara JE, Feng B, Johnson K, Gu S, Gennert MA, King MA. Motion capture of chest and abdominal markers using a flexible multi-camera motion-tracking system for correcting motion-induced artifacts in cardiac SPECT. In: Proceedings of the 2007 nuclear science symposium conference record, NSS'07. IEEE; 2007. p. 4289–93.
[11] Coupier J, Hamoudi S, Telese-Izzi S, Feipel V, Rooze M, Van Sint Jan S. A novel method for in-vivo evaluation of finger kinematics including definition of healthy motion patterns. Clin Biomech (Bristol, Avon) 2016;31:47–58.
[12] Leardini A, Chiari L, Della Croce U, Cappozzo A. Human movement analysis using stereophotogrammetry. Part 3. Soft tissue artifact assessment and compensation. Gait Posture 2005;21:212–25.
[13] Shultz R, Kedgley AE, Jenkyn TR. Quantifying skin motion artifact error of the hindfoot and forefoot marker clusters with the optical tracking of a multi-segment foot model using single-plane fluoroscopy. Gait Posture 2011;34:44–8.
[14] Birch I, Deschamps K. Quantification of skin marker movement at the malleoli and Talar heads. J Am Podiatr Med Assoc 2011;101:497–504.

[15] Nester C, Jones RK, Liu A, Howard D, Lundberg A, Arndt A, et al. Foot kinematics during walking measured using bone and surface mounted markers. J Biomech 2007;40:3412–23.
[16] Kalra MK, Maher MM, Toth TL, Hamberg LM, Blake MA, Shepard JA, et al. Strategies for CT radiation dose optimization. Radiology 2004;230:619–28.
[17] Brenner DJ, Hall EJ. Computed tomography – an increasing source of radiation exposure. N Engl J Med 2007;357:2277–84.
[18] Biswas D, Bible JE, Bohan M, Simpson AK, Whang PG, Grauer JN. Radiation exposure from musculoskeletal computerized tomographic scans. J Bone Joint Surg Am 2009;91:1882–9.
[19] Goo HW. CT radiation dose optimization and estimation: an update for radiologists. Korean J Radiol 2012;13:1–11.
[20] Dobbe JGG, de Roo MGA, Visschers JC, Strackee SD, Streekstra GJ. Evaluation of a quantitative method for carpal motion analysis using clinical 3D and 4D CT protocols. IEEE Trans Med Imaging 2019;38:1048–57.
[21] Yi JW, Park HJ, Lee SY, Rho MH, Hong HP, Choi YJ, et al. Radiation dose reduction in multidetector CT in fracture evaluation. Br J Radiol 2017;90:20170240.
[22] Tuijthof GJ, Beimers L, Jonges R, Valstar ER, Blankevoort L. Accuracy of a CT-based bone contour registration method to measure relative bone motions in the hindfoot. J Biomech 2009;42:686–91.
[23] Tuijthof GJ, Zengerink M, Beimers L, Jonges R, Maas M, van Dijk CN, et al. Determination of consistent patterns of range of motion in the ankle joint with a computed tomography stress-test. Clin Biomech (Bristol, Avon) 2009;24:517–23.
[24] Stebbins J, Harrington M, Thompson N, Zavatsky A, Theologis T. Repeatability of a model for measuring multi-segment foot kinematics in children. Gait Posture 2006;23:401–10.
[25] Saraswat P, MacWilliams BA, Davis RB. A multi-segment foot model based on anatomically registered technical coordinate systems: method repeatability in pediatric feet. Gait Posture 2012;35:547–55.
[26] Leardini A, Benedetti MG, Berti L, Bettinelli D, Nativo R, Giannini S. Rear-foot, mid-foot and fore-foot motion during the stance phase of gait. Gait Posture 2007;25:453–62.
[27] Dobbe JGG, Strackee SD, Schreurs AW, Jonges R, Carelsen B, Vroemen JC, et al. Computer-assisted planning and navigation for corrective distal radius osteotomy, based on pre- and intraoperative imaging. IEEE Trans Bio-Med Eng 2011;58:182–90.
[28] Ibánes L, Schroeder W. The insight segmentation and registration toolkit, software guide. Kitware Inc; 2003.
[29] Carelsen B, Jonges R, Strackee SD, Maas M, van Kemenade P, Grimbergen CA, et al. Detection of in vivo dynamic 3-D motion patterns in the wrist joint. IEEE Trans Biomed Eng 2009;56:1236–44.
[30] Lorensen WE, Cline HE. Marching cubes: a high resolution 3D surface construction algorithm. SIGGRAPH Comput Graph 1987;21:163–9.
[31] Nelder JA, Mead R. A simplex method for function minimization. Comput J 1965;7:308–13.
[32] Kuo H-Y, Su H-R, Lai S-H, Wu C-C. 3D object detection and pose estimation from depth image for robotic bin picking. In: Proceedings of the 2014 IEEE international conference on automation science and engineering (CASE). IEEE; 2014. p. 1264–9.
[33] Girden ER. ANOVA: repeated measures. Sage; 1992.
[34] Merriaux P, Dupuis Y, Boutteau R, Vasseur P, Savatier X. A study of vicon system positioning performance. Sensors (Basel) 2017:17.
[35] Kainz H, Carty CP, Maine S, Walsh HPJ, Lloyd DG, Modenese L. Effects of hip joint centre mislocation on gait kinematics of children with cerebral palsy calculated using patient-specific direct and inverse kinematic models. Gait Posture 2017;57:154–60.
[36] Zemp R, List R, Gulay T, Elsig JP, Naxera J, Taylor WR, et al. Soft tissue artefacts of the human back: comparison of the sagittal curvature of the spine measured using skin markers and an open upright MRI. PLoS One 2014;9:e95426.